PHYSICAL REVIEW A VOLUME 50, NUMBER 3 SEPTEMBER 1994

Ionization of an excited hydrogen atom by a high-frequency circularly polarized pulsed field

Mariusz Gajda* and Bernard Piraux
Institut de Physique, Université Catholique de Louvain, 2, Chemin du Cyclotron, B1348 Louvain-La-Neuve, Belgium

Kazimierz Rzążewski
Centrum Fizyki Teoretycznej Polskiej Akademii Nauk, Al. Lotników 32/46, 02-668 Warszawa, Poland

(Received 11 March 1994; revised manuscript received 12 May 1994)

We study the ionization of atomic hydrogen by a high-frequency circularly polarized field. We solve numerically the time-dependent Schrödinger equation for the atomic wave function, which beforehand is expanded in a Coulomb-Sturmian basis. We analyze the ionization from various initial states differing by their azimuthal quantum number m, the principal and the angular quantum numbers being equal to 2 and 1, respectively. At high field intensities we observe important differences in the ionization yield: strong stabilization is observed for $m = 0$ and $m = 1$ while for $m = -1$ the atom is almost completely ionized. We also study the electron energy spectra for the same cases and show that they are characterized by a multiple splitting of the above-threshold-ionization (ATI) peaks. The behavior of the ionization yield as well as the structure observed in the ATI spectra are explained in terms of the ac-Stark shift and width of the atomic levels. We also consider some of the aspects of the underlying dynamics by means of a very simple essential-state model.

PACS number(s): 32.80.Rm

I. INTRODUCTION

The interaction of simple atomic systems with very strong laser pulses has become a subject of intensive experimental and theoretical investigation. Laser pulses currently produced in the laboratory generate electric fields which often exceed the atomic internal binding field. This has led to the observation of new and rather unexpected phenomena such as, for example, the above-threshold ionization (ATI), the generation of very high harmonics of the driving field, and multielectron ionization of atoms and molecules. A review of the present understanding of these processes is found in [1]. Recently, various numerical simulations have indicated that a one-electron atomic system may become stable against ionization while exposed to a very strong laser pulse. This means that there exists a regime of very high peak field intensity in which the ionization yield decreases with increasing peak field intensity. This stabilization process is presently studied both theoretically [2] and experimentally [3] when the laser field is linearly polarized. The aim of the present paper is to investigate the atomic stabilization problem for a circularly polarized light.

Nonperturbative solution of the time-dependent Schrödinger equation is a difficult numerical problem. For linearly polarized light, the problem has an axial symmetry and as a result is two dimensional. This leads to a substantial simplification of numerical efforts involved. By contrast, the case of a circularly polarized light is much more difficult since it is truly three dimensional. So far, only a few papers [4,5] have treated this problem.

The existence of an additional degree of freedom in the case of circularly polarized light is of course related to the nonconservation of the z component of the angular momentum in the optical transitions. This leads to some new interesting features of the ionization process. In the linear case, the azimuthal quantum number does not change when the photon is absorbed. Therefore, an electron can reach the continuum via the $s \to p \to s$ transitions, i.e., its angular momentum can remain relatively small. If this is the case, the electron penetrates the nucleus region very easily. In this region the effective interaction with the external field is very strong and the probability for the atom to ionize can be quite large. For the circular polarization (say σ^+, for instance), the selection rules require an increase of the atomic azimuthal quantum number by one, $m \to m+1$, each time the photon is absorbed. This leads to an increase of electron's angular momentum giving rise to a large centrifugal barrier. This barrier prevents the electron from strong penetration of the nucleus region.

Ionization of atomic hydrogen by a high-frequency circularly polarized pulse has already been considered but, to our knowledge, the atom was always assumed to be in its ground state [5]. By contrast, ionization from a highly excited state has been studied theoretically in the microwave regime. In that case, it was shown by means of a classical treatment [6] that the probability of ionization from Rydbergs orbits depends drastically on the z projection of the angular momentum.

In our paper we study the ionization of hydrogen atom by a strong circularly polarized laser pulse. We pay

---

*Permanent address: Institute of Physics, Polish Academy of Sciences, Al. Lotników 32/46, 02-668 Warsaw, Poland.

particular attention to the difference between ionization from initial atomic states which differ by their azimuthal quantum number. For this reason we study the ionization from the $(n = 2, l = 1, m = 0, \pm 1)$ states, where n is the principal quantum number and l and m the angular momentum and azimuthal quantum numbers, respectively. In our calculations we assume the photon energy to be two times larger than the ionization potential. In this case the absorption of a single photon brings the electron high in the continuum. We study in details the ionization probability as a function of the peak laser intensity as well as the electron energy spectrum.

The paper is organized as follows. A brief description of our numerical treatment is presented in Sec. II. In Sec. III we present the results for the ionization yields and the electron energy spectra. In Sec. IV these results are explained and some aspects of the underlying dynamics are discussed within a very simple essential-state model. Our final conclusions are presented in Sec. V. Unless explicitly stated, we use atomic units throughout.

II. FORMALISM

In order to study the interaction of atomic hydrogen with a strong circularly polarized laser pulse, we consider the following time-dependent Schrödinger equation:

$$i\frac{\partial}{\partial t}\Psi(\mathbf{r},t) = [H_0 + \mathbf{A}(t)\cdot\mathbf{p}]\Psi(\mathbf{r},t), \tag{1}$$

where H_0 is the atomic Hamiltonian and $\mathbf{A}(t)$ is the vector potential associated with the field $\boldsymbol{\mathcal{E}}(t) = -\partial\mathbf{A}(t)/\partial t$. In Eq. (1) we use the dipole approximation. We omit the $\mathbf{A}^2$-term since within this approximation it only introduces a constant phase. In order to describe the pulsed field, we assume the following form of the vector potential:

$$\mathbf{A}(t) = A_0 f(t)[-\mathbf{e}_x \sin(\omega t) + \mathbf{e}_y \cos(\omega t)]. \tag{2}$$

In this formula A_0 is the amplitude of the potential, ω is the frequency of the laser light, $\mathbf{e}_x$ and $\mathbf{e}_y$ are the unit vectors in the x and y directions, respectively, and $f(t)$ is a slowly varying envelope. In our calculations, we assume that $f(t)$ has a sine-square form

$$f(t) = \sin^2(\pi t/t_d), \tag{3}$$

where t_d is the pulse time duration.

The form of vector potential (2) corresponds to the σ^+ or σ^- polarization depending on the sign of ω. If the initial state is an eigenstate of a given azimuthal number, Eq. (1) is invariant under a simultaneous change of the sign of ω and m. For this reason, and without any loss of generality, we assume that the field has a σ^+ polarization.

The solution of Eq. (1) has to be found numerically. Actually, there are two basic methods of solution to this problem. One is simply the direct integration of the partial differential Eq. (1) using a grid method [2]. The other possibility consists in representing the Schrödinger equation in a basis of L^2-integrable functions; we then obtain a set of coupled first-order differential equations to solve for the expansion coefficients [7]. An appropriate choice of the basis leads to a sparse matrix representation of the total Hamiltonian; this may significantly reduce the numerical effort in terms of storage and execution time. The close link between the Coulomb-Sturmian functions $S^{\kappa}_{n,l}$ [8] and the atomic hydrogen radial functions suggests that it is convenient to expand the total wave function as follows:

$$\Psi(\mathbf{r},t) = \sum_{n,l,m} a_{nlm}(t)\frac{1}{r}S^{\kappa}_{n,l}(r)Y_{l,m}(\theta,\phi), \tag{4}$$

where κ is an arbitrary parameter. The Coulomb-Sturmian functions may be expressed in terms of the radial wave functions $R_{n,l}(r/n)$ for the bound states of atomic hydrogen:

$$S^{\kappa}_{n,l}(r) = N_{n,l}R_{n,l}(\kappa r), \tag{5}$$

with $N_{n,l}$ a normalization constant. In order to appreciate the advantages and the limits of the present method, let us briefly review the main properties of the Coulomb-Sturmian functions and the expansion (4):

(i) The Coulomb-Sturmian functions form a discrete and complete set in the space of L^2-integrable functions. These functions are not orthogonal since the corresponding overlap matrix is tridiagonal.

(ii) The κ parameter distinguishes between different sets of Coulomb-Sturmian functions. Since in practice we take into account a finite number, say N, of basis functions, we actually need two parameters κ and N to specify our basis. For a given value of N and κ we obtain N eigenvalues of the atomic Hamiltonian. Some of these eigenvalues correspond to the negative energies of atomic hydrogen while others correspond to positive energies. It is possible to choose κ and N such that a given number of these negative eigenvalues are correctly reproduced and at the same time such that the distribution of the positive energies covers a given energy range depending on the physical situation.

(iii) Both the atomic and the interaction Hamiltonian can be very easily expressed in our Sturmian basis: first, all the matrix elements have a very simple analytical expression and second, the total Hamiltonian matrix is very sparse. It is in fact block tridiagonal, the diagonal blocks being tridiagonal and the off-diagonal blocks four-diagonal. As a result, if the number of the basis functions is equal to N, the number of independent nonzero elements is of the order of $7 \times N \ll N^2$.

(iv) If we study the ionization process, we have to properly describe not only bound spectrum wave functions but also the scattering Coulomb wave functions. Within our approach, the continuum spectrum is discretized (only a finite number of positive eigenenergies of the atomic Hamiltonian is taken into account). In practice, it means that for a given energy, the corresponding radial scattering Coulomb wave function is correctly described by a linear superposition of Coulomb-Sturmian functions up to a certain distance only. Beyond this point the positive energy wave function (4) drops exponentially to zero. By an appropriate choice of N and κ, we can make this distance large enough. A similar problem arises also within the space-time grid integration method. The space grid is always finite and it has to be sufficiently large in order to avoid an unphysical "reflection" of the outgoing wave from the boundary of the grid. In the implementation of the present method we paid special attention to this problem making sure that this reflection does not occur. Within the grid method, this reflection problem is avoided by introducing an "absorber" at the boundary of the grid. Within our approach, we can overcome this problem by complex rotating the total Hamiltonian. In this way, the time-evolution operator becomes nonunitary since its continuum component decays exponentially in time. In other words, that means that the probability density flux dies out at large distances as is the case in the presence of an absorber at large distance [8]. It is important to note that, in general, the number of Coulomb-Sturmian functions to be included is significantly smaller when the total Hamiltonian is complex rotated since it is only close to the nucleus that the total wavefunction has to be precisely described. In the present case, the results have been obtained without complex rotation of the total Hamiltonian; we have, however, checked that the same results can also be obtained with a complex rotation of the Hamiltonian.

(v) The hydrogen free-free dipole matrix elements have a singular component. Because the radial Coulomb-Sturmian functions simulate the Coulomb wave function in some finite area only, all dipole matrix elements are finite in this basis. By using a Coulomb-Sturmian expansion of the total wave function we therefore simultaneously introduce a prescription for the regularization of the free-free dipole elements.

In the Coulomb-Sturmian basis, Eq. (1) transforms into a set of first-order differential equations for the expansion coefficients $a_{n,l,m}(t)$. The matrix of the system is sparse so we avoid the storage problem. On the other hand, this system of equations is stiff. To overcome this difficulty we use a diagonally implicit fourth-order Runge-Kutta method [9] for the time propagation. At the end of the propagation, we get the expansion coefficients of the wave function $\Psi(\mathbf{r}, t_d)$ in the Coulomb-Sturmian basis. The projection of this solution on the atomic basis gives us the amplitudes $b_{E,l,m}$. If the energy E is equal to $E = -1/2n^2$, $|b_{E,l,m}|^2$ represents the probability for the system to be in the hydrogenic bound state of quantum numbers (n, l, m). If E_i and E_{i+1} are two consecutive positive energies, $|b_{E_{i+1},l,m}|^2$ represents the probability for the system to be in the continuum and to have the energy E between E_i and E_{i+1}. Therefore, the electron spectrum which is a probability density can be defined as follows:

$$P(E) = \sum_{l,m} \frac{|b_{E_{i+1},l,m}|^2}{E_{i+1} - E_i}, \qquad E_i < E \leq E_{i+1}. \qquad (6)$$

III. RESULTS

In our calculations we studied the ionization of hydrogen atom from a state $(n = 2, l = 1, m)$ by a field of σ^+ polarization. In this paper, we restrict our analysis to the case of large photon frequencies, namely, we chose the laser frequency to be equal to $\omega = 0.25$, which corresponds to a photon energy large enough to bring the electron high into the continuum. The pulse duration is equal to 20 optical cycles ($t_d = 40\pi/\omega$). The size of the Coulomb-Sturmian basis is adjusted according to the pulse peak intensity and varies from $N = 2500$ for low field intensities up to $N = 14\,000$ for superintense fields. More precisely we use a set of functions $S^{\kappa}_{n,l}$ where n ranges up to 250 and l up to 5 in the simplest case; in the extreme case, n ranges up to 500 and l up to 8.

Before describing our results for the ionization yields and the electron energy spectra, let us stress that the electric field experienced by an electron on a $n = 2$ orbit is equal to $\mathcal{E} = 0.0625$ in atomic units. Since in our calculations we study the ionization of the atom by electric fields ranging from 0 to 0.75, it is clear that in most of the cases, the peak electric field will exceed the binding field by a large factor.

The ionization probability from the $(n = 2, l = 1, m = -1)$ initial state is presented in Fig. 1(a). Initially, for small electric fields, the ionization probability grows linearly with intensity; then it reaches its maximum for electric fields around 0.3. Clearly there is no sign of real stabilization in this case. By contrast, the behavior of the ionization yield changes significantly when atomic hydrogen is initially in the $(n = 2, l = 1, m = 0)$ state; as shown in Fig. 1(b), the ionization yield reaches its maximum for a smaller field. Moreover, it exhibits a clear stabilization behavior for fields larger than 0.3. Even more interesting is the behavior of the ionization yield when atomic hydrogen is initially in the $(n = 2, l = 1, m = 1)$ state; in addition to the stabilization regime, which also occurs for electric fields larger than 0.3, we observe in Fig. 1(c) a stability window around $\mathcal{E} = 0.1$. At this stage it is interesting to wonder to what extend the significant differences observed in the ionization yields will also manifest themselves in the electron energy spectra.

For moderately small electric fields ($\mathcal{E} = 0.0625$), all the spectra exhibit one well pronounced ATI peak (the next ones being very small) independently on the azimuthal quantum number of the initial state; this is illustrated in Figs. 2–4. However, we observe a structure in the first ATI peak in the case where atomic hydrogen is ionized from the $(n = 2, l = 1, m = 1)$ state. For higher electric fields ($\mathcal{E} = 0.125$), more ATI peaks appear (see Figs. 5–7) and we clearly notice the development of a very rich structure in the first ATI peak [10] when again the azimuthal quantum number of the initial state is $m = 1$. Our results for higher field intensities ($\mathcal{E} = 0.25$) are presented in Figs. 8–10. First, we observe a broadening of each ATI peak. Second, the ATI peak splitting, which occurs at lower field intensity when the azimuthal quantum number m of the initial state of atomic hydrogen is equal to 1, starts to develop also when $m = 0$. In the case where $m = 1$ (see Fig. 10), each ATI peak splits into two well pronounced subpeaks with very rich fine structures. Finally, when the electric field becomes very large ($\mathcal{E} = 0.75$), the electron energy spectra exhibit very complicated structures for all values of m as it is clearly indicated in Figs. 11–13.

All these results clearly indicate that underlying dynamics depend very strongly on the value of the azimuthal quantum number of the initial state of atomic hydrogen. The substantial differences that are observed in the ionization yields and the electron energy spectra will be explained in the following section in terms of the ac-Stark shift and width of the atomic levels.

IV. INTERPRETATION OF THE RESULTS

In presence of the external laser field, the atomic levels are shifted and broadened. The most appropriate analysis of this dressing effect is based on a Floquet approach

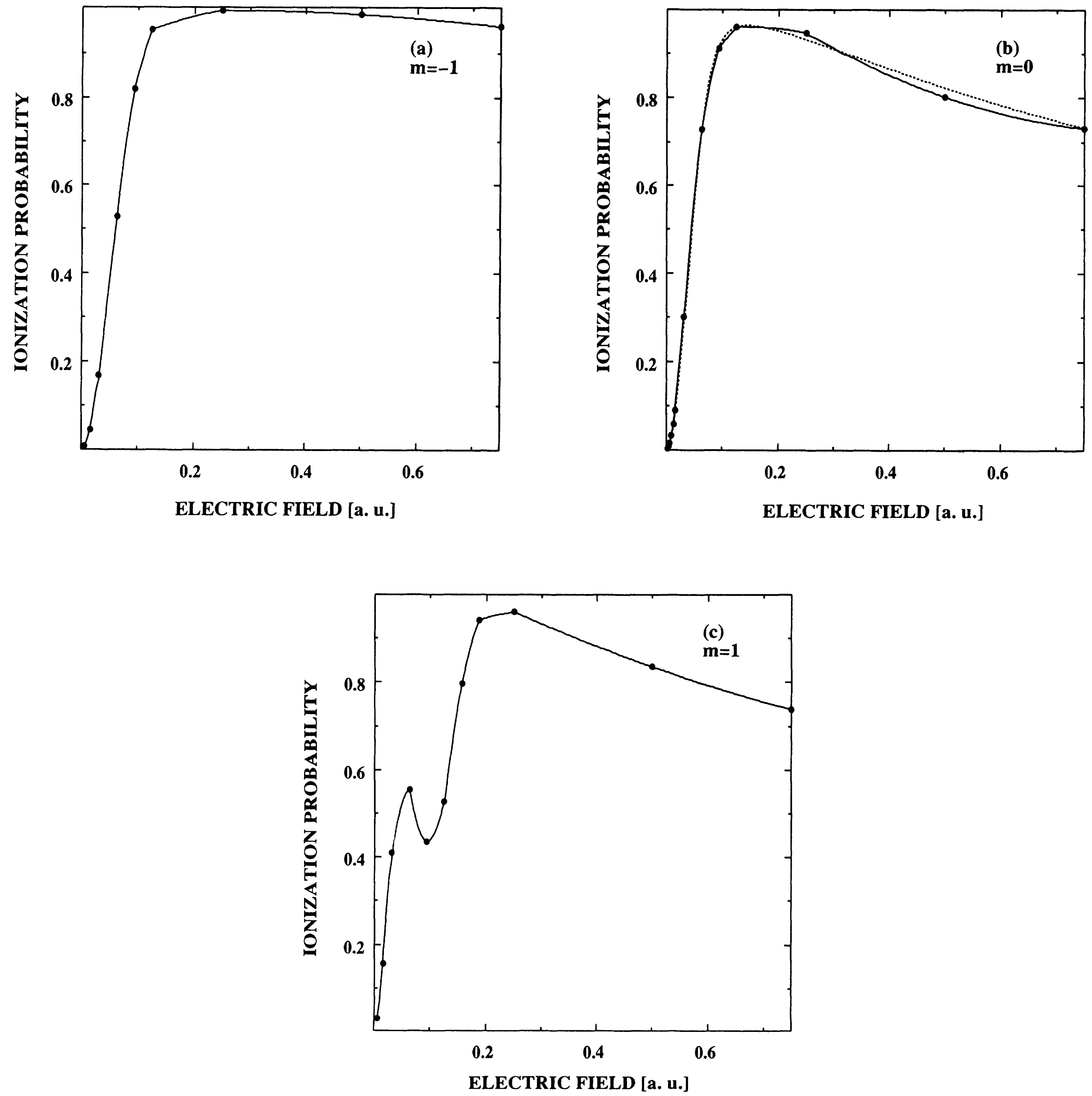

FIG. 1. Ionization probability from the $(n = 2, l = 1, m)$ state as a function of the peak electric field. The pulse has a sine-square profile, its duration is equal to 20 optical cycles, and the photon energy is $\omega = 0.25$ a.u. (a) $m = -1$; (b) $m = 0$, the solid line corresponds to the numerical simulation, and the dashed line corresponds to the essential state model described in the following part of the paper; (c) $m = +1$.

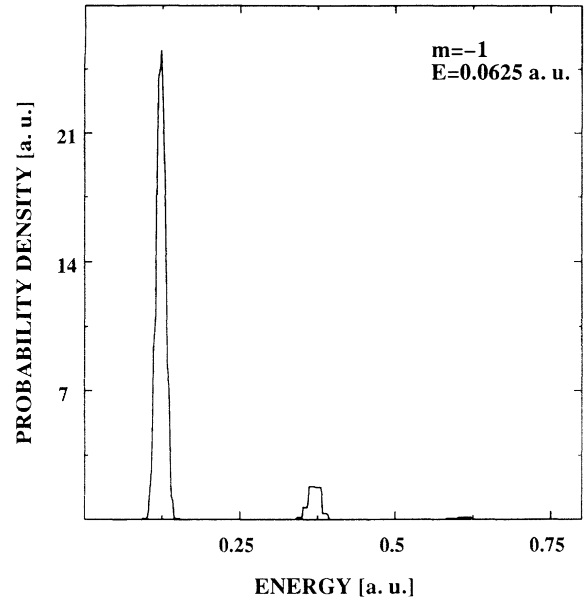

FIG. 2. Electron energy spectrum produced when atomic hydrogen initially in the ($n = 2, l = 1, m = -1$) state interacts with a sine-square pulse of duration equal to 20 optical cycles and single photon energy $\omega = 0.25$ a.u. The peak electric field is equal to $\mathcal{E} = 0.0625$ a.u.

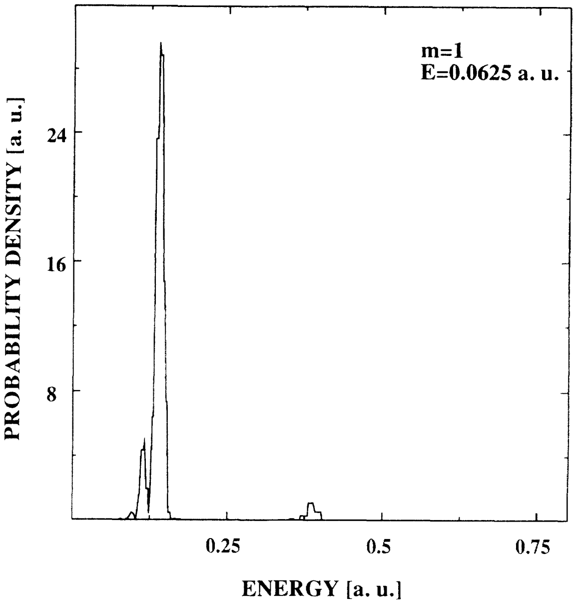

FIG. 4. Electron energy spectrum produced when atomic hydrogen initially in the ($n = 2, l = 1, m = +1$) state interacts with a sine-square pulse of duration equal to 20 optical cycles and single photon energy $\omega = 0.25$ a.u. The peak electric field is equal to $\mathcal{E} = 0.0625$ a.u.

[11]; however, a simple second-order calculation gives already some qualitative estimate of the shifts. In the case of a circularly polarized field, this quadratic shift strongly depends on the value of the azimuthal quantum number of each atomic state [12]. Our results for these shifts are presented in Figs. 14(a), 15(a), and 16(a). We want to point out once more that these results have only a qualitative character and are valid only for relatively small electric field strength. Let us stress at this stage that what is represented is the second-order contribution to the shift of the $\mathbf{A} \cdot \mathbf{p}$ term [see Eq. (1)]. Since the $\mathbf{A}^2$ term (within the dipole approximation) adds a constant

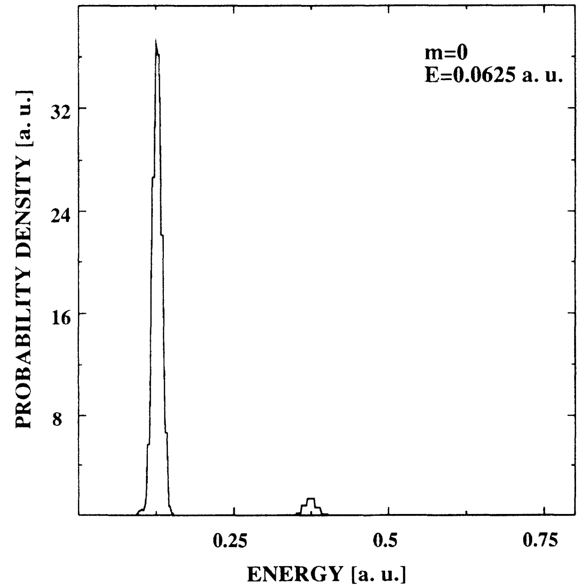

FIG. 3. Electron energy spectrum produced when atomic hydrogen initially in the ($n = 2, l = 1, m = 0$) state interacts with a sine-square pulse of duration equal to 20 optical cycles and single photon energy $\omega = 0.25$ a.u. The peak electric field is equal to $\mathcal{E} = 0.0625$ a.u.

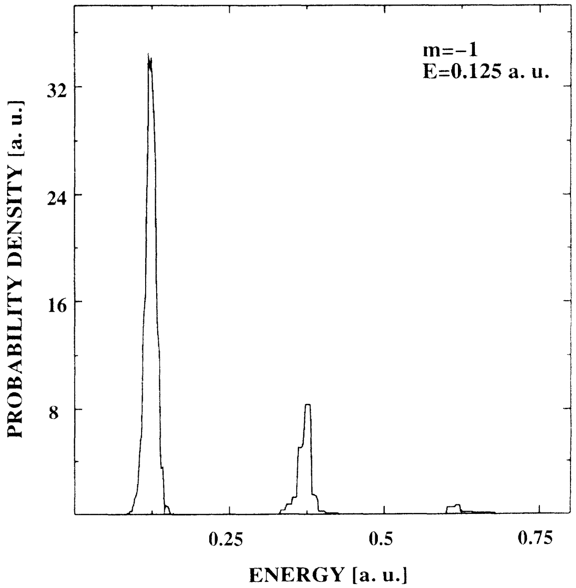

FIG. 5. Electron energy spectrum produced when atomic hydrogen initially in the ($n = 2, l = 1, m = -1$) state interacts with a sine-square pulse of duration equal to 20 optical cycles and single photon energy $\omega = 0.25$ a.u. The peak electric field is equal to $\mathcal{E} = 0.125$ a.u.

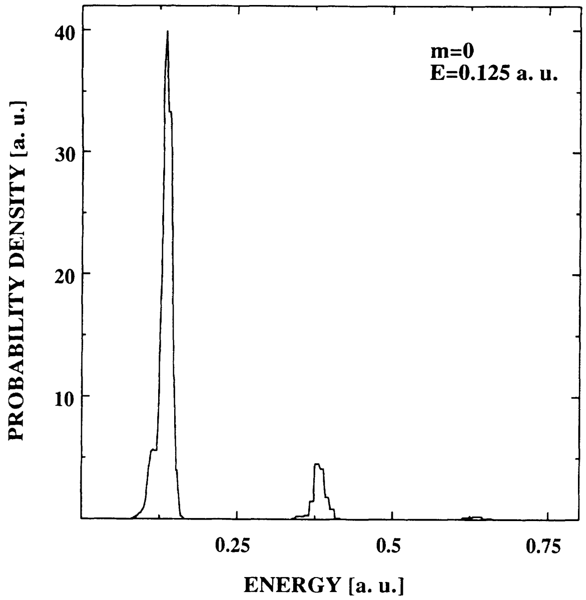

FIG. 6. Electron energy spectrum produced when atomic hydrogen initially in the ($n = 2, l = 1, m = 0$) state interacts with a sine-square pulse of duration equal to 20 optical cycles and single photon energy $\omega = 0.25$ a.u. The peak electric field is equal to $\mathcal{E} = 0.125$ a.u.

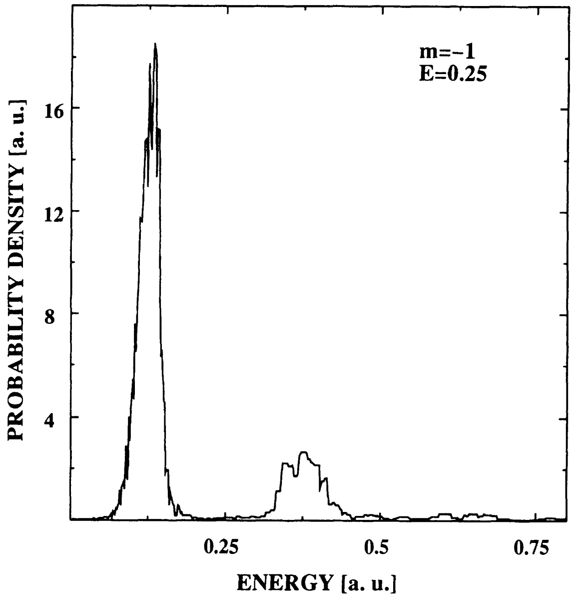

FIG. 8. Electron energy spectrum produced when atomic hydrogen initially in the ($n = 2, l = 1, m = -1$) state interacts with a sine-square pulse of duration equal to 20 optical cycles and single photon energy $\omega = 0.25$ a.u. The peak electric field is equal to $\mathcal{E} = 0.25$ a.u.

shift, we do not take it into account; this is consistent with Eq. (1). In other words, our zero on the energy scale is the continuum threshold.

The shifts of the atomic levels characterized by $l = 1$ and $m = -1$ [see Fig. 14(a)] are negative, but stay very small even for very strong fields. By contrast, for m different from -1, the shifts become positive and all levels cross even at moderately high field [13], as is shown in Figs. 15(a) and 16(a). For comparison, energies of the ($n = 2, l = 1, m = \pm 1$) states obtained with the help of the Floquet approach are given in Fig. 17. These results have been obtained by Potvliege [19] and by his

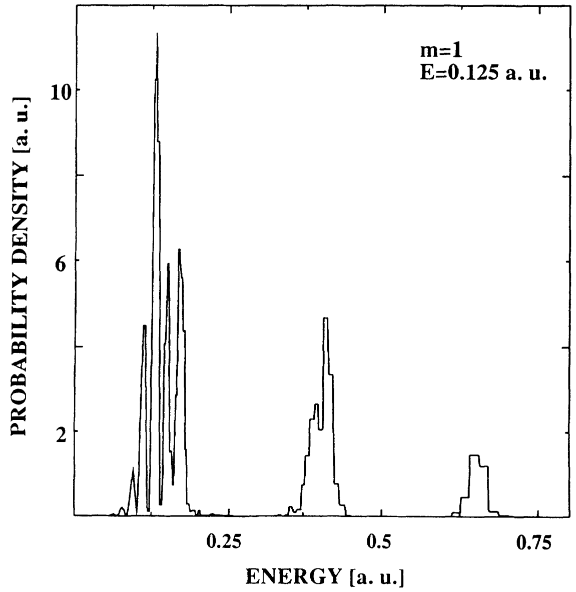

FIG. 7. Electron energy spectrum produced when atomic hydrogen initially in the ($n = 2, l = 1, m = +1$) state interacts with a sine-square pulse of duration equal to 20 optical cycles and single photon energy $\omega = 0.25$ a.u. The peak electric field is equal to $\mathcal{E} = 0.125$ a.u.

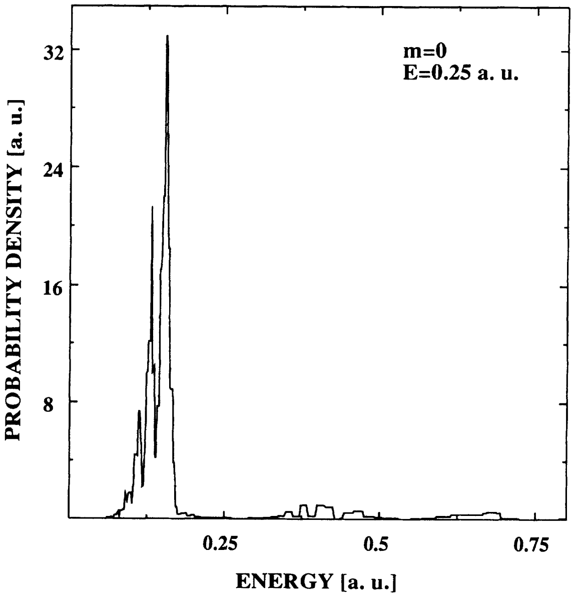

FIG. 9. Electron energy spectrum produced when atomic hydrogen initially in the ($n = 2, l = 1, m = 0$) state interacts with a sine-square pulse of duration equal to 20 optical cycles and single photon energy $\omega = 0.25$ a.u. The peak electric field is equal to $\mathcal{E} = 0.25$ a.u.

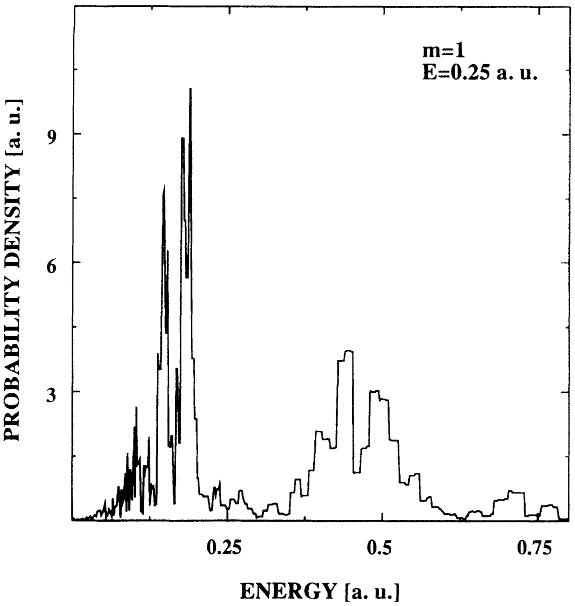

FIG. 10. Electron energy spectrum produced when atomic hydrogen initially in the $(n = 2, l = 1, m = +1)$ state interacts with a sine-square pulse of duration equal to 20 optical cycles and single photon energy $\omega = 0.25$ a.u. The peak electric field is equal to $\mathcal{E} = 0.25$ a.u.

courtesy we are permitted to present them in this paper. For the strong electric field we observe the large departure from the second-order ac-Stark shift; however, for the field strength smaller than 0.1 the agreement (even quantitative) is remarkable; the $m = 1$ and $m = 0$ states are shifted upward while $m = -1$ state is shifted downward.

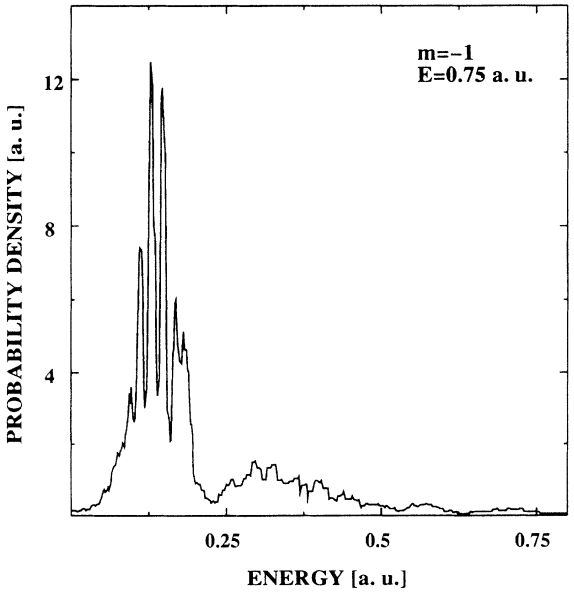

FIG. 11. Electron energy spectrum produced when atomic hydrogen initially in the $(n = 2, l = 1, m = -1)$ state interacts with a sine-square pulse of duration equal to 20 optical cycles and single photon energy $\omega = 0.25$ a.u. The peak electric field is equal to $\mathcal{E} = 0.75$ a.u.

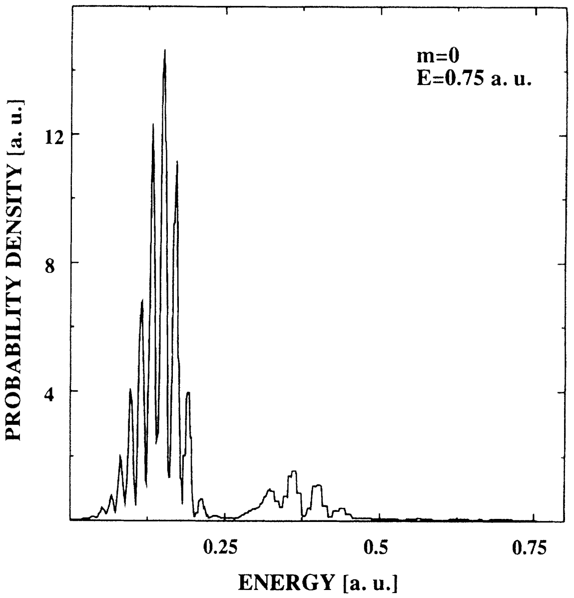

FIG. 12. Electron energy spectrum produced when atomic hydrogen initially in the $(n = 2, l = 1, m = 0)$ state interacts with a sine-square pulse of duration equal to 20 optical cycles and single photon energy $\omega = 0.25$ a.u. The peak electric field is equal to $\mathcal{E} = 0.75$ a.u.

We expect that the differences observed in the behavior of the shift of the atomic levels for increasing field intensities have a strong influence on the dynamics of the ionization process. When, for instance, two levels are close together they might be strongly coupled by a two-photon Raman transition (since the angular momentum of all these levels is the same). This is clearly illustrated

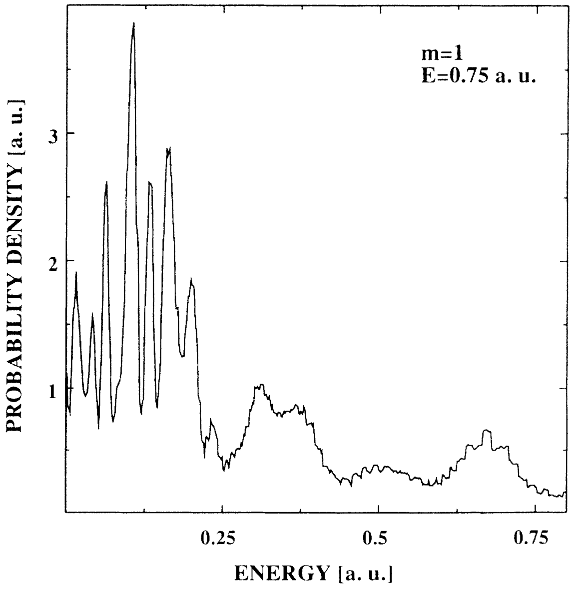

FIG. 13. Electron energy spectrum produced when atomic hydrogen initially in the $(n = 2, l = 1, m = +1)$ state interacts with a sine-square pulse of duration equal to 20 optical cycles and single photon energy $\omega = 0.25$ a.u. The peak electric field is equal to $\mathcal{E} = 0.75$ a.u.

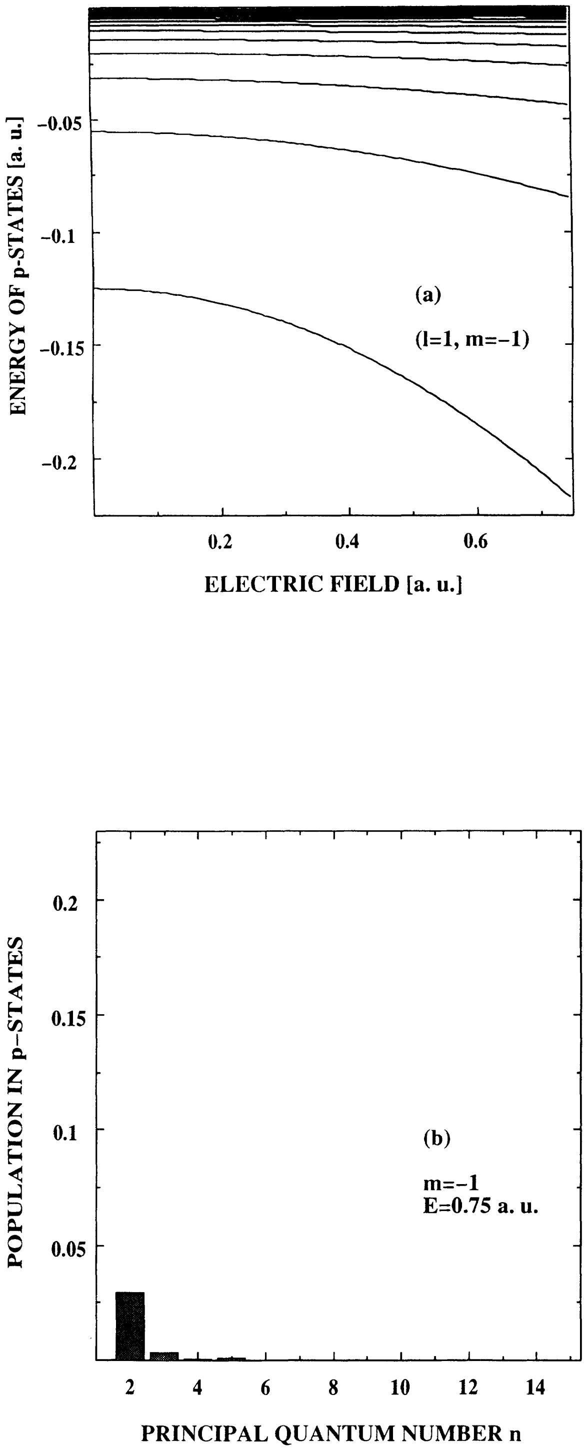

FIG. 14. (a) Energy of atomic hydrogen levels of angular quantum numbers equal to ($l = 1, m = -1$). Quadratic ac-Stark shift resulting from the interaction with the circularly polarized (σ^+ polarization) field of frequency $\omega = 0.25$ a.u. is taken into account. The different lines correspond to the consecutive principal quantum numbers $n = 2, 3, \ldots$. (b) Population of atomic hydrogen levels of angular quantum numbers equal to ($l = 1, m = -1$) after the interaction with the circularly polarized (σ^+ polarization) sine-square pulse of duration equal to 20 optical cycles, single photon energy $\omega = 0.25$ a.u., and peak electric field $\mathcal{E} = 0.75$ a.u. Initially the total population was in the ($n = 2, l = 1, m = -1$) state.

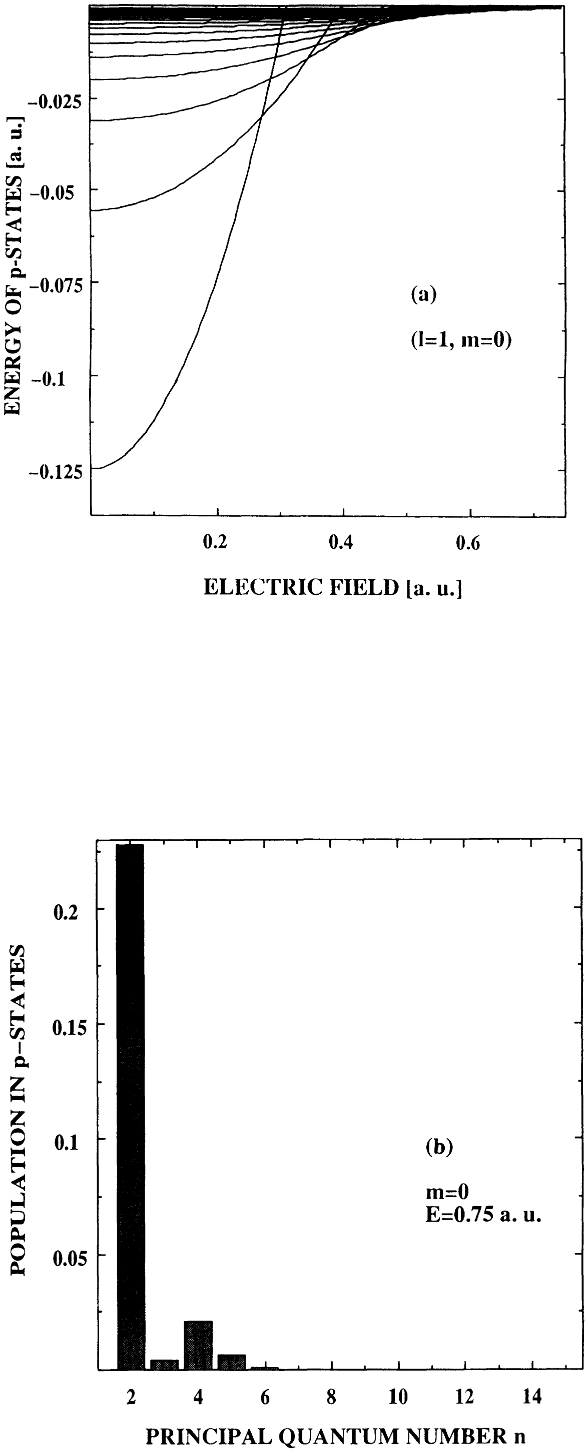

FIG. 15. (a) Energy of atomic hydrogen levels of angular quantum numbers equal to ($l = 1, m = 0$). Quadratic ac-Stark shift resulting from the interaction with the circularly polarized (σ^+ polarization) field of frequency $\omega = 0.25$ a.u. is taken into account. The different lines correspond to the consecutive principal quantum numbers $n = 2, 3, \ldots$. (b) Population of atomic hydrogen levels of angular quantum numbers equal to ($l = 1, m = 0$) after the interaction with the circularly polarized (σ^+ polarization) sine-square pulse of duration equal to 20 optical cycles, single photon energy $\omega = 0.25$ a.u., and peak electric field $\mathcal{E} = 0.75$ a.u. Initially the total population was in the ($n = 2, l = 1, m = 0$) state.

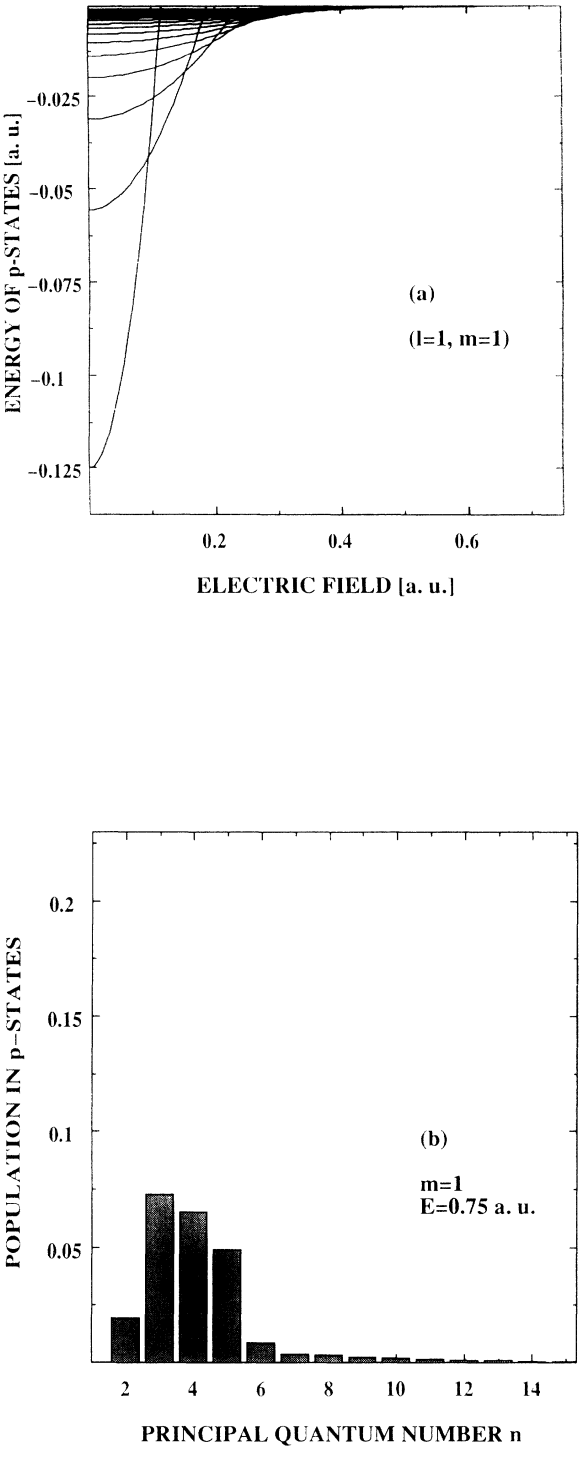

FIG. 16. (a) Energy of atomic hydrogen levels of angular quantum numbers equal to ($l = 1, m = +1$). Quadratic ac-Stark shift resulting from the interaction with the circularly polarized (σ^+ polarization) field of frequency $\omega = 0.25$ a.u. is taken into account. The different lines correspond to the consecutive principal quantum numbers $n = 2, 3, \ldots$. (b) Population of atomic hydrogen levels of angular quantum numbers equal to ($l = 1, m = +1$) after the interaction with the circularly polarized (σ^+ polarization) sine-square pulse of duration equal to 20 optical cycles, single photon energy $\omega = 0.25$ a.u., and peak electric field $\mathcal{E} = 0.75$ a.u. Initially the total population was in the ($n = 2, l = 1, m = 1$) state.

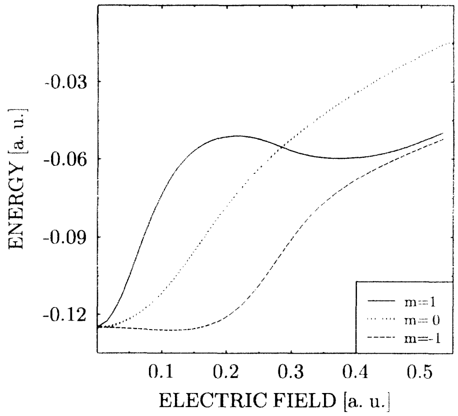

FIG. 17. Floquet energies (the real part) of the ($n = 2, l = 1, m = 0, \pm 1$) states as a function of the amplitude of the circularly polarized electric field (σ^+ polarization) of frequency $\omega = 0.25$ a.u.

in Figs. 14(b), 15(b), and 16(b) where we show the populations left in various atomic levels after the interaction with the pulse, the peak electric field being in all three cases fixed and equal to 0.75. When initially, the population is in the ($n = 2, l = 1, m = -1$) state, we do not observe [see Fig. 14(b)] any significant transfer of population toward higher excited states. This is of course expected since level separation increases with intensity. When the azimuthal quantum number of the initial state is equal to 0, level separation decreases with increasing field; as a result, some population is transferred to the nearest states [see Fig. 15(b)]. This effect is even more pronounced when the azimuthal quantum number of the initial state is equal to 1, as is shown in Fig. 16(b).

These results indicate that the occurrence of a stabilization regime at high field intensity when the azimuthal quantum number m of the initial state is equal to 0 or 1 is a consequence of the formation of a coherent superposition of excited atomic levels of the same parity of the initial state. A similar stabilization mechanism has been proposed by Fedorov and Movsesian [14] and Parker and Stroud [15]. This stabilization mechanism is expected to be really efficient when the atom is initially in a high lying Rydberg state. However, a recent calculation in the case of a linearly polarized field has shown that it is not necessarily true [16]. To our knowledge, the present numerical simulation seems to be the first one that confirms the importance of this stabilization process. At first sight, this is unexpected since in the present case, the atom is initially in a low lying state. However, the role of the shift of each atomic level is crucial here since, for various field intensities, the separation of these levels might become of the same order of magnitude as their total energy width, which includes both the ionization width and the pulse bandwidth. In our case, the frequency bandwidth of the pulse is relatively large (of the order of 0.002). However, we expect that for longer pulse, a similar effect could occur provided that the initial state is a higher excited state; this follows from our analysis of the shift of the levels. Finally, according to the present discussion, it is not surprising to see that the stability window [17] observed for $m = +1$ occurs at a value of the electric field at which the $(n = 2, l = 1, m = 1)$ state crosses the $(n = 3, l = 1, m = 1)$ state. Similarly, the stabilization regime for $m = 0$ starts also for an electric field in the vicinity of such a crossing.

In order to gain more insight into the dynamics, and in particular to understand the origin of the multiple splitting of the ATI peaks, we study in the following a simple essential state model which includes only two bound states (of the same parity) and only one continuum (of opposite parity). Although very simple, the model describes the most important physical process involved, namely, the Raman coupling of the two bound states via the continuum. We expect that this model will give a good qualitative description of the physics when the azimuthal quantum number m of the initial state is equal to 0, but not when $m = +1$ since the number of states which participate to the dynamics is much larger. Under the above condition, the equations for the amplitudes read

$$\frac{d}{dt}\alpha_1(t) = -i\left(\omega_1 + \delta_1\frac{[\mathcal{E}(t)]^2}{\omega^2}\right)\alpha_1(t) -i\mathcal{E}(t)d_1\int\beta(\epsilon,t)d\epsilon, \tag{7}$$

$$\frac{d}{dt}\alpha_2(t) = -i\left(\omega_2 + \delta_2\frac{[\mathcal{E}(t)]^2}{\omega^2}\right)\alpha_2(t) -i\mathcal{E}(t)d_2\int\beta(\epsilon,t)d\epsilon, \tag{8}$$

$$\frac{d}{dt}\beta(\epsilon,t) = -i\epsilon\beta(\epsilon,t) - i\mathcal{E}(t)[d_1\alpha_1(t) + d_2\alpha_2(t)], \tag{9}$$

where $\mathcal{E}(t)$ is the oscillating (with frequency ω) electric field whose amplitude follows the sine-square envelope given by Eq. (3); $\alpha_1(t)$ and $\alpha_2(t)$ are the amplitudes of $(n = 2, l = 1, m = 0)$ and $(n = 3, l = 1, m = 0)$ states of negative energies ω_1 and ω_2, respectively. $\beta(\epsilon, t)$ is the amplitude of positive energy state $(\epsilon, l = 2, m = 1)$; d_1 and d_2 are the bound-free dipole matrix elements and $\delta_1[\mathcal{E}(t)]^2/\omega^2$ and $\delta_2[\mathcal{E}(t)]^2/\omega^2$ are the quadratic ac-Stark shifts of the bound states. Before proceeding with the calculations, let us describe and discuss the main assumptions of our model.

(i) The bound-free dipole matrix elements d_1 and d_2 do not depend on the energy of the final state; this assumption can only be justified for large kinetic energies of the outgoing electron.

(ii) Only one continuum is included in these calculations; therefore, free-free transitions are neglected and only the first ATI peak is described. Other peaks may appear, but in this case they must correspond to higher-order transitions within the same continuum.

(iii) Since the photon energy is much larger than the ionization potential, the integration over ϵ in Eqs. (7) and (8) is extended from minus to plus infinity. As a result, the electron energy spectrum extends from negative to positive energies. Because ω_1 and ω_2 are very small compared to the "typical" value of ω (which is the photon frequency) it follows from Eqs. (7)–(9) that the electron energy spectrum will be quasisymmetric with respect to the energy threshold. We therefore expect that the height of the ATI peak will be reduced by a factor 2.

The formal integration of Eq. (9)

$$\beta(\epsilon,t) = -\frac{i}{\sqrt{\pi}}\int^t e^{i\epsilon t'}\mathcal{E}(t')\left[\sqrt{\gamma_1}\alpha_1(t') + \sqrt{\gamma_2}\alpha_2(t')\right]dt' \tag{10}$$

allows us to eliminate the continuous spectrum from Eqs. (7) and (8). After the following substitution:

$$\gamma_1 = \pi d_1^2, \qquad \gamma_2 = \pi d_2^2, \tag{11}$$

Eqs. (7) and (8) transform into a closed set of coupled equations which may be written as follows:

$$\frac{d}{dt}\alpha_1 = -i\left[\omega_1 + \mathcal{E}^2\left(\frac{\delta_1}{\omega^2} - i\gamma_1\right)\right]\alpha_1 - \mathcal{E}^2\sqrt{\gamma_1\gamma_2}\alpha_2, \tag{12}$$

$$\frac{d}{dt}\alpha_2 = -i\left[\omega_2 + \mathcal{E}^2\left(\frac{\delta_2}{\omega^2} - i\gamma_2\right)\right]\alpha_2 - \mathcal{E}^2\sqrt{\gamma_1\gamma_2}\alpha_1. \tag{13}$$

δ_1, δ_2, γ_1, and γ_2 are the parameters of the model. The ionization probability is equal to

$$P = 1 - (|\alpha_1|^2 + |\alpha_2|^2) \tag{14}$$

and the electron energy spectrum is defined as

$$S(\epsilon) = |\beta(\epsilon, t \to \infty)|^2, \tag{15}$$

The parameters of the model are fitted in such a way that the model reproduces as well as possible the ionization yield obtained by means of our numerical simulation [see the dashed line in Fig. 1(b)]. It is important to stress that the shifts $\delta_1\mathcal{E}^2/\omega^2$ and $\delta_2\mathcal{E}^2/\omega^2$ are of the order of second-order ac-Stark shifts. At low field intensities, $\gamma_1\mathcal{E}^2$ and $\gamma_2\mathcal{E}^2$ may be interpreted as the widths of the bound states involved in the model. This of course is not true any more at very high field intensity.

Having fitted these parameters, let us now analyze the electron energy spectra. Those are presented in Figs. 18–20 for various values of the peak electric field, the azimuthal quantum number of the initial state being equal to 0 as previously mentioned. First of all, as we expect, only the first ATI peak is reproduced and as indicated before, its height is smaller by almost a factor 2. Second, there is a remarkable qualitative agreement between the spectra calculated within the model and the numerical simulation. We clearly see that for increasing peak field strength, a fine structure of the first ATI peak develops.

At this stage, it is important to realize that two types of mechanisms may lead to the occurrence of this multipeak structure. The first mechanism involves the interference of each bound state contribution to the amplitude $\beta(\epsilon, t)$ [see Eq. (10)]. The second mechanism involves the interference between the ionization amplitude β produced at the same intensity on the rising and falling edge of the pulse. Both mechanisms depend on the laser intensity as well as the pulse duration. As it is shown in [18], the distance between the subpeaks produced by the

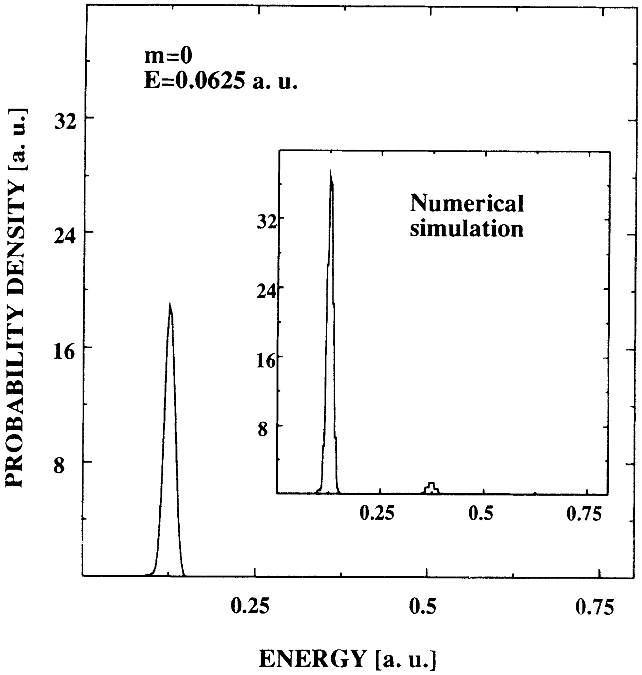

FIG. 18. Result of the model calculation for the electron energy spectrum produced when atomic hydrogen initially in the $(n = 2, l = 1, m = 0)$ state interacts with a sine-square pulse of duration equal to 20 optical cycles and single photon energy $\omega = 0.25$ a.u. The peak electric field is equal to $\mathcal{E} = 0.0625$ a.u. For comparison, the corresponding result of numerical simulation is shown.

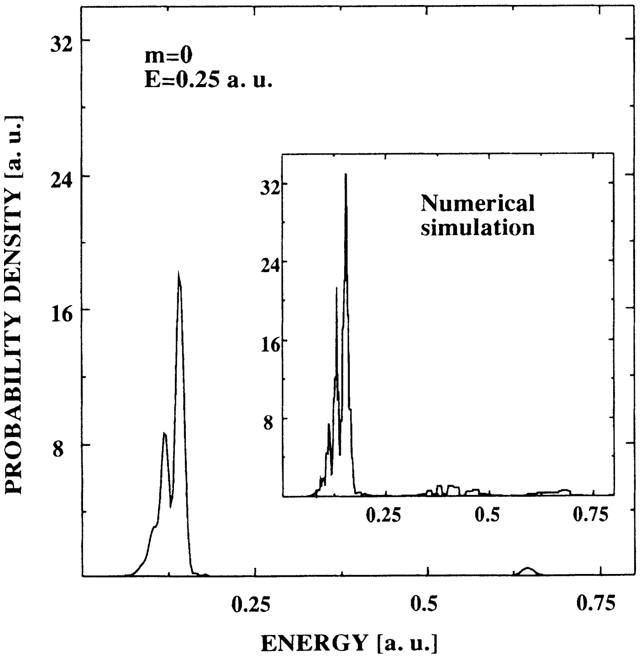

FIG. 19. Result of the model calculation for the electron energy spectrum produced when atomic hydrogen initially in the $(n = 2, l = 1, m = 0)$ state interacts with a sine-square pulse of duration equal to 20 optical cycles and single photon energy $\omega = 0.25$ a.u. The peak electric field is equal to $\mathcal{E} = 0.25$ a.u. For comparison, the corresponding result of numerical simulation is shown.

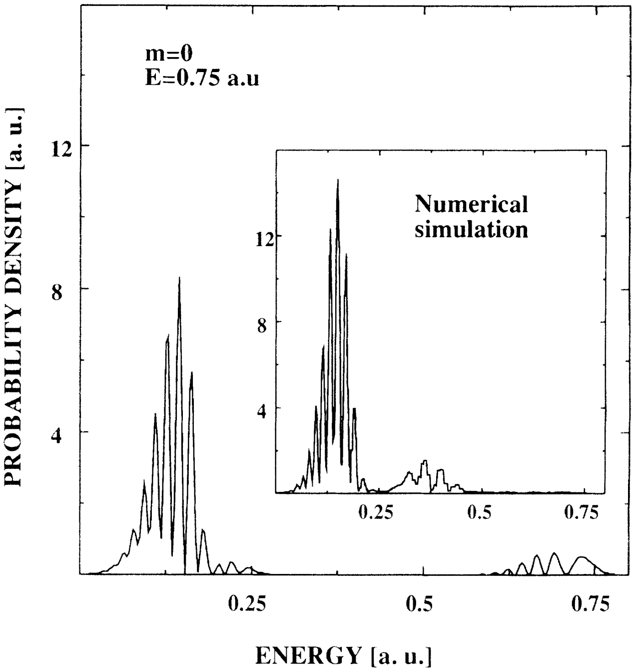

FIG. 20. Result of the model calculation for the electron energy spectrum produced when atomic hydrogen initially in the $(n = 2, l = 1, m = 0)$ state interacts with a sine-square pulse of duration equal to 20 optical cycles and single photon energy $\omega = 0.25$ a.u. The peak electric field is equal to $\mathcal{E} = 0.75$ a.u. For comparison, the corresponding result of numerical simulation is shown.

second mechanism is proportional to $\mathcal{E}^{2/3}$. As a result, at low field intensity, any kind of well pronounced multipeak structure in the ATI spectrum will be hardly attributed to this mechanism. Therefore, the comparison between the electron energy spectra produced by the same pulsed field interacting with atomic hydrogen initially in various states $(n = 2, l = 1, m = -1, 0, +1)$ (see Figs. 5–7) rather suggests that the splitting observed in Fig. 7 results from the first mechanism.

V. CONCLUSIONS

We have studied the interaction of atomic hydrogen initially in a $(n = 2, l = 1, m = -1, 0, +1)$ state with a circularly polarized high-frequency pulsed electric field. We have solved numerically the corresponding time-dependent Schrödinger equation; this is carried out first by expanding the total wave function in a basis of Coulomb-Sturmian functions and then by propagating the amplitudes in time by means of a high-order diagonally implicit method.

We have shown that both the ionization yields and the electron energy spectra are very sensitive to the azimuthal quantum number of the initial state. When $m = 0, +1$ atomic hydrogen stabilizes at high field intensity while for $m = -1$ it ionizes almost completely. Moreover, we have demonstrated that when $m = 1$ the first ATI peaks of the electron energy spectra are characterized by a splitting into many subpeaks. This structure is also present when $m = 0$, but for higher peak electric fields.

The dependence of the ionization yields and the electron energy spectra on the azimuthal quantum number of the initial state of atomic hydrogen has been explained in terms of both the shift and the width of the atomic levels. When $m = +1$, we have shown that the shift of each level becomes very important, leading to many level crossings. These crossings are responsible for the trapping a significant part of the total population into a coherent superposition of various states close and of the same parity as the initial state. At high field intensity, this superposition is stable against ionization. This process, which actually involves interferences between various ionization amplitudes, leads to the multipeak structure observed in the ATI spectra. This stabilization mechanism has been previously proposed by Fedorov and Movsesian [14]. However, to our knowledge, no numerical simulation has so far demonstrated that this mechanism is really effective in producing a substantial stabilization of the atom, the present physical conditions are the first encountered ones in which it is the case.

ACKNOWLEDGMENTS

M.G. and K.R. acknowledge financial support of the Polish Government Grant No. 2 P 30212504; they also thank the Catholic University of Louvain for having given them the opportunity to visit the Physics Department at various occasions and for long periods. B.P. received support from Fonds National de la Recherche Scientifique de Belgique. We are very grateful to R.M. Potvliege for computing the Floquet energies of atomic states relevant for our analysis.

---

[1] For the review see the special issue of Laser Phys. **3**, 219 (1993); K.C. Kulander, K.J. Schafer, and J.L. Krause, in *Atoms in Strong Radiation Fields*, edited by M. Gavrila (Academic, Boston, 1992), p. 247; see also in *Super-Intense Laser Atom Physics*, Vol. 316 of *NATO Advanced Study Institute, Series B: Physics*, edited by B. Piraux, A. L'Huillier, and K. Rzążewski (Plenum Press, New York, 1994).

[2] K.C. Kulander, K.J. Schafer, and J.L. Krause, Phys. Rev. Lett. **66**, 2601 (1991).

[3] R.R. Jones and P.H. Bucksbaum, Phys. Rev. Lett. **67**, 3215 (1991).

[4] J. Zakrzewski, D. Delande, J.C. Gay, and K. Rzążewski, Phys. Rev. A **47**, R2468 (1993).

[5] M. Horbatsch, Phys. Lett. A **165**, 58 (1992); M. Pont and M. Gavrila, Phys. Rev. Lett. **65**, 2362 (1990).

[6] K. Rzążewski and B. Piraux, Phys. Rev. A **47**, R1612 (1993).

[7] E. Huens and B. Piraux, Phys. Rev. A **47**, R1568 (1993).

[8] See, e.g., M. Rotenberg, Adv. At. Mol. Phys. **6**, 233 (1970).

[9] E. Hairer and G. Wanner, *Solving Ordinary Differential Equations II: Stiff and Differential-Algebraic Problems* (Springer-Verlag, Berlin, 1991).

[10] The resolution obtained for the electron energy spectrum depends on both the number N of Sturmian functions in the basis and the κ parameter. We adjust N and κ in order to get the highest possible density of positive eigenenergies of the atomic Hamiltonian around the expected position of the first ATI peak.

[11] For a review of Floquet methods, see S.-I. Chu, Adv. At. Mol. Phys. **21**, 197 (1985). Floquet-type calculations to treat the interaction of atomic hydrogen with a strong field have been carried out recently by many authors; see, for example, R.M. Potvliege and R. Shakeshaft, Phys. Rev. A **38**, 1098 (1988).

[12] A.M. Bonch-Bruevich and V.A. Khodovoi, Usp. Fiz. Nauk **93**, 71 (1967).

[13] The quadratic shift for $m = 1$ is large because the coupling of the ground state with the $(n = 2, l = 1, m = 1)$ state is very large when the field has a σ^+ polarization. However, we should keep in mind that a more rigorous Floquet calculation is necessary to obtain precise values of the actual shift.

[14] M.V. Fedorov and A.M. Movsesian, J. Opt. Soc. Am. B **6**, 928 (1989).

[15] J. Parker and C.R. Stroud, Jr., Phys. Rev. A **40**, 5651 (1989).

[16] A. Scrinzi, N. Elander, and B. Piraux, Phys. Rev. A **48**, R2527 (1993).

[17] The concept of stability window has been discussed previously in a different context by L. Dimou and F.H.M. Faisal, Phys. Rev. A **46**, 4442 (1992).

[18] J.N. Bardsley, A. Szöke, and M.J. Comella, J. Phys. B **21**, 3899 (1988); V.C. Reed and K. Burnett, Phys. Rev. A **43**, 6217 (1991).

[19] The results for the energies of Floquet states have been computed and made available to us by courtesy of R.M. Potvliege. For results of Floquet calculations of shifts and widths of the 1s and 2s energy levels of atomic hydrogen irradiated by intense circularly polarized light see M. Dörr, R.M. Potvliege, D. Proulx, and R. Shakeshaft, Phys. Rev. A **43**, 3729 (1991); for higher Floquet states see also R.M. Potvliege and P.H.G. Smith, *Super-Intense Laser-Atom Physics* (Ref. [1]), p. 173.

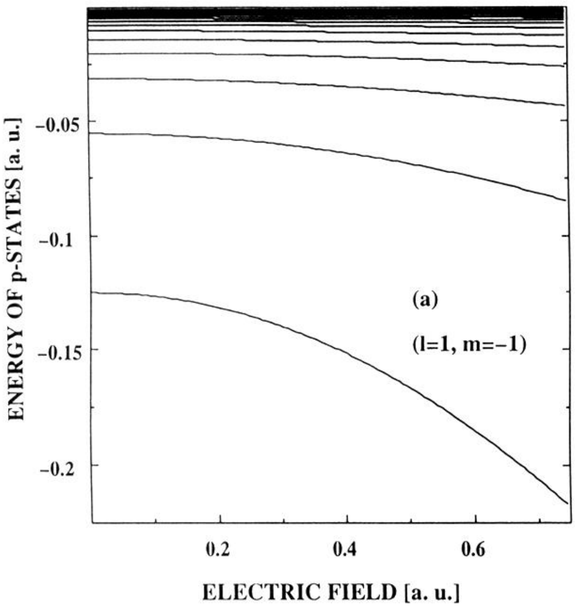

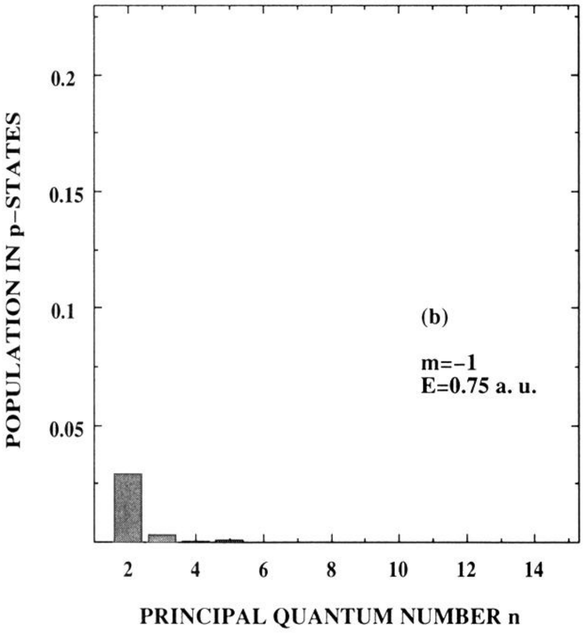

FIG. 14. (a) Energy of atomic hydrogen levels of angular quantum numbers equal to $(l = 1, m = -1)$. Quadratic ac-Stark shift resulting from the interaction with the circularly polarized (σ^+ polarization) field of frequency $\omega = 0.25$ a.u. is taken into account. The different lines correspond to the consecutive principal quantum numbers $n = 2, 3, \ldots$. (b) Population of atomic hydrogen levels of angular quantum numbers equal to $(l = 1, m = -1)$ after the interaction with the circularly polarized (σ^+ polarization) sine-square pulse of duration equal to 20 optical cycles, single photon energy $\omega = 0.25$ a.u., and peak electric field $\mathcal{E} = 0.75$ a.u. Initially the total population was in the $(n = 2, l = 1, m = -1)$ state.

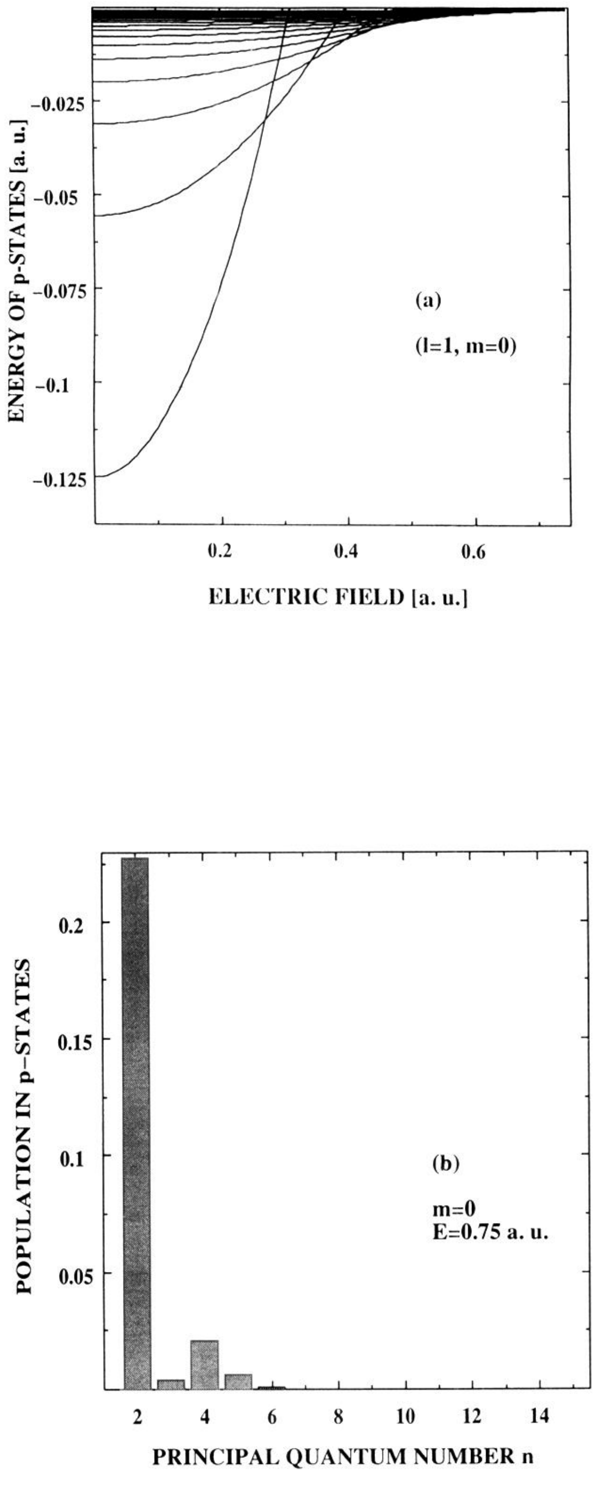

FIG. 15. (a) Energy of atomic hydrogen levels of angular quantum numbers equal to $(l = 1, m = 0)$. Quadratic ac-Stark shift resulting from the interaction with the circularly polarized (σ^+ polarization) field of frequency $\omega = 0.25$ a.u. is taken into account. The different lines correspond to the consecutive principal quantum numbers $n = 2, 3, \ldots$. (b) Population of atomic hydrogen levels of angular quantum numbers equal to $(l = 1, m = 0)$ after the interaction with the circularly polarized (σ^+ polarization) sine-square pulse of duration equal to 20 optical cycles, single photon energy $\omega = 0.25$ a.u., and peak electric field $\mathcal{E} = 0.75$ a.u. Initially the total population was in the $(n = 2, l = 1, m = 0)$ state.

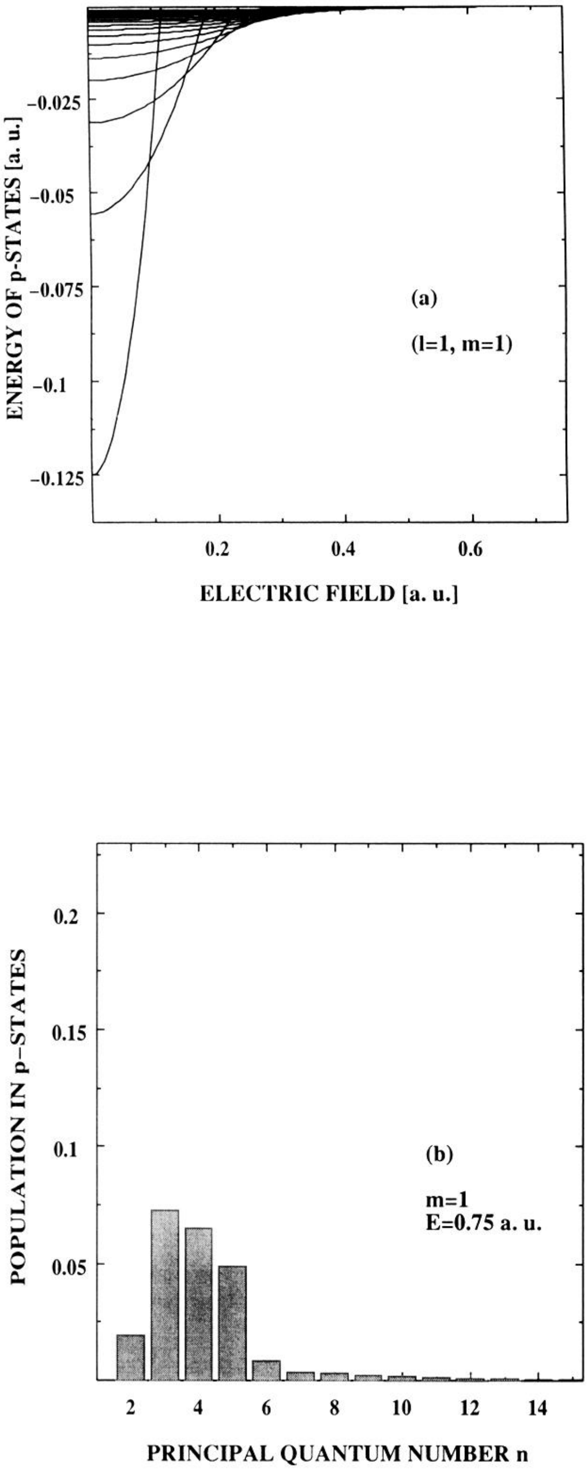

FIG. 16. (a) Energy of atomic hydrogen levels of angular quantum numbers equal to $(l = 1, m = +1)$. Quadratic ac-Stark shift resulting from the interaction with the circularly polarized (σ^+ polarization) field of frequency $\omega = 0.25$ a.u. is taken into account. The different lines correspond to the consecutive principal quantum numbers $n = 2, 3, \ldots$. (b) Population of atomic hydrogen levels of angular quantum numbers equal to $(l = 1, m = +1)$ after the interaction with the circularly polarized (σ^+ polarization) sine-square pulse of duration equal to 20 optical cycles, single photon energy $\omega = 0.25$ a.u., and peak electric field $\mathcal{E} = 0.75$ a.u. Initially the total population was in the $(n = 2, l = 1, m = 1)$ state.